

## **Effect of use of methyltriethylammonium chloride individually and combined with n-butylamine on the characteristics of the ZSM-12 zeolite crystallization process**

**Efeito do uso do cloreto de metiltriethylamônio individualmente e combinado com n-butilamina nas características do processo de cristalização da zeólita ZSM-12**

**Efecto del uso de cloruro de metiltriethylamonio individualmente y combinado con n-butilamina sobre las características del proceso de cristalización de zeolita ZSM-12**

Received: 01/05/2022 | Reviewed: 01/10/2022 | Accept: 01/12/2022 | Published: 01/14/2022

**Elisa Gabriela Costa Gouveia**

ORCID: <https://orcid.org/0000-0002-5532-9677>

Universidade Federal de Alagoas, Brasil

E-mail: [elisa.gouveia@ctec.ufal.br](mailto:elisa.gouveia@ctec.ufal.br)

**Soraya Lira Alencar**

ORCID: <https://orcid.org/0000-0001-5945-5809>

Universidade Federal de Alagoas, Brasil

E-mail: [soraya.alencar@copeve.ufal.br](mailto:soraya.alencar@copeve.ufal.br)

**Bruno José Barros da Silva**

ORCID: <https://orcid.org/0000-0002-0297-9588>

Universidade Federal de Alagoas, Brasil

E-mail: [brunojbarros@hotmail.com](mailto:brunojbarros@hotmail.com)

**Maritza Montoya Urbina**

ORCID: <https://orcid.org/0000-0001-8335-3124>

Universidade Federal de Alagoas, Brasil

E-mail: [maritza@ctec.ufal.br](mailto:maritza@ctec.ufal.br)

**Julyane da Rocha Santos Solano**

ORCID: <https://orcid.org/0000-0002-0942-469X>

Universidade Federal de Alagoas, Brasil

E-mail: [julyane.rocha@hotmail.com](mailto:julyane.rocha@hotmail.com)

**Antonio Osimar Sousa da Silva**

ORCID: <https://orcid.org/0000-0002-6524-8571>

Universidade Federal de Alagoas, Brasil

E-mail: [antonio.silva@ctec.ufal.br](mailto:antonio.silva@ctec.ufal.br)

### **Abstract**

The improvement of the structure of the ZSM-12 zeolite has been extensively studied, due to its shape selectivity properties, acidity and hydrothermal stability, with this zeolite being used in a wide range of applications, such as adsorbent, ion exchanger and in important reactions in the petrochemical area. In this work, the effect on the crystallization characteristics and physicochemical properties of the ZSM-12 zeolite using methyltriethylammonium chloride, individually, and combined with n-butylamine, as structure-directing agent was studied. The syntheses were carried out at 160 and 170 °C between 48 and 144 h in static medium. The samples obtained were characterized by the techniques of X-ray diffraction, thermal analysis, nitrogen adsorption-desorption and temperature-programmed ammonia desorption. The simultaneous use of methyltriethylammonium chloride and n-butylamine, at a ratio of 0.2, promoted the obtainment of highly crystalline ZSM-12, with an increase in the microporous area and acidity, denoting an improvement in the physicochemical properties of this zeolite.

**Keywords:** ZSM-12 zeolite; Structure-directing agent; Methyltriethylammonium chloride; n-butylamine; Physicochemical properties.

### **Resumo**

O aprimoramento da estrutura da zeólita ZSM-12 vem sendo extensivamente estudado, devido às suas propriedades de seletividade de forma, acidez e estabilidade hidrotérmica, sendo esta zeólita utilizada em uma ampla gama de aplicações, tais como adsorvente, trocador iônico e em importantes reações na área petroquímica. Neste trabalho o efeito sob as características da cristalização e das propriedades físico-químicas da zeólita ZSM-12 utilizando o cloreto de metiltriethylamônio, individualmente, e combinado com n-butilamina, como agente direcionador de estrutura foi estudado. As sínteses foram realizadas a 160 e 170 °C entre 48 e 144 h em meio estático. As amostras obtidas foram caracterizadas pelas técnicas de difratometria de raios X, análises térmicas, adsorção-dessorção de nitrogênio e dessorção de amônia a temperatura programada. A utilização simultânea do cloreto de metiltriethylamônio e n-

butilamina, na razão 0,2, promoveu a obtenção da ZSM-12 altamente cristalina, com incremento da área microporosa e acidez, denotando uma melhoria das propriedades físico-químicas desta zeólita.

**Palavras-chave:** Zeólita ZSM-12; Agente direcionador de estrutura; Cloreto de metiltriethylamônio; n-butilamina; Propriedades físico-químicas.

### Resumen

La mejora de la estructura de la zeolita ZSM-12 ha sido ampliamente estudiada, debido a sus propiedades de selectividad de forma, acidez y estabilidad hidrotermal. Esta zeolita se utiliza en una amplia gama de aplicaciones, como adsorbente, intercambiador de iones y en reacciones importantes. en el área petroquímica. En este trabajo se estudió el efecto sobre las características de cristalización y propiedades fisicoquímicas de la zeolita ZSM-12 utilizando cloruro de metiltriethylamonio, individualmente y combinado con n-butilamina, como agente director de estructura. Las síntesis se realizaron a 160 y 170 °C entre 48 y 144 h en medio estático. Las muestras obtenidas se caracterizaron mediante las técnicas de difracción de rayos X, análisis térmico, adsorción-desorción de nitrógeno y desorción de amoníaco programada por temperatura. El uso simultáneo de cloruro de metiltriethylamonio y n-butilamina, en una proporción de 0,2, promovió la obtención de ZSM-12 altamente cristalino, con aumento del área microporosa y acidez, lo que denota una mejora en las propiedades fisicoquímicas de esta zeolita.

**Palabras clave:** Zeolita ZSM-12; Agente director de estructura; Cloruro de metiltriethylamonio; n-butilamina; Propiedades fisicoquímicas.

## 1. Introduction

Since the development of the first synthetic zeolites between 1940 (Barrer, 1948) and 1950 (Milton, 1959), the improvement on the synthesis process of these materials has been attracting continuous interest in the academic and industrial spheres, as these materials have controllable acidity, high surface area, high thermal and hydrothermal stability, enabling the use of these structures in a wide range of applications, such as adsorbents (Rodeghero et al., 2019; Cao et al., 2021), ion exchangers (Figueiredo et al., 2018; Kwon et al., 2021) and catalysts in the fine chemical and petrochemical industries (Kosareva et al., 2021; Imyen et al., 2021).

Among these structures, ZSM-12 (MTW-type structure) is a zeolite with high silica content, having a system of one-dimensional channels that do not intersect. Its pores are ellipse-shaped and constituted by 12-member rings (12-MR) with opening dimensions of 5,6 x 6,1 Å. Due to these structural characteristics, ZSM-12 has a high shape selectivity in obtaining sterically unimpeded linear molecules (Kulikov et al., 2019). Particularly, ZSM-12 is used as catalyst in the selective production of p-xylene (Glotov et al., 2021), 2,6-dimethylnaphthalene (Li et al., 2011), p-tert-butylphenol (Li et al., 2014), 4,4'-diisopropylbiphenyl (Chokkalingam et al., 2013), in the cracking (Sanhoob et al., 2018) and hydrocracking of hydrocarbons (Mehla et al., 2013).

The synthesis of the ZSM-12 zeolite was first reported by Rosinski and Rubin (1974) using tetraalkylammonium cations as structure-directing agent (SDA). ZSM-12 is usually synthesized from quaternary ammonium salts, which are involved in the formation of the aluminosilicate porous structure and affect the characteristics of the resulting material. Thus, a significant number of reports have focused on the study of nucleation and growth of crystals of this zeolite in the presence of various organic ammonium salts, such as methyltriethylammonium and N,N-dimethyl-N-ethyl(monoethanol)ammonium (Kulikov et al., 2019), tetraethylammonium (Toktarev & Ione, 1997; Kasunič et al., 2009), trimethylethylammonium (Počkaj et al., 2018), imidazole, pyridine and piperidine salts (Kore, R. & Srivastava, 2012), and diquaternary ammonium salts (Moini et al.; 1994; Han et al., 2005; Veselý et al., 2019).

The simultaneous use of two structure-directing agents in the synthesis of zeolite structures, in many cases, becomes a promising methodology as it allows the optimization of the physicochemical properties of the zeolite (Chen et al., 2018), by obtaining different pore systems (Holland et al., 1999; Lee et al., 2014), controlling morphology and modification of adsorption amount (Margarit et al., 2015; Masoumifard et al., 2016) or changing the composition of the intended zeolite phase (Wang et al., 2009; Rani et al., 2016). Methyltriethylammonium chloride (MTEACl) is described as an effective structure-

directing agent to synthesize ZSM-12 (Silva et al., 2017). On the other hand, n-butylamine, which is a low-cost amine, is rarely reported to be applied as SDA in the ZSM-12 synthesis.

Based on Chen et al. (2018), who explored the use of isopropylamine and pyrrolidine, simultaneously, as SDAs in the synthesis of zeolite ZSM-23, this manuscript aimed to explore the effect of applying methyltriethylammonium chloride (MTEACl), individually, and combined with n-butylamine (n-But) as structure-directing agents on the crystallization process and on the physicochemical properties of zeolite ZSM-12.

## 2. Methodology

### 2.1 Synthesis of ZSM-12 zeolite

The ZSM-12 zeolite synthesis methodology adopted was based on Silva et al. (2017), where the precursor reagents were added in stoichiometric proportions in order to obtain a mixture with the following molar composition:  $x$  MTEACl :  $y$  n-But : 12.5 Na<sub>2</sub>O : 1 Al<sub>2</sub>O<sub>3</sub> : 100 SiO<sub>2</sub> : 2500 H<sub>2</sub>O, with  $x = 15, 20$  and  $25$ ,  $y = 0, 20$  and  $30$ . The preparation of the reaction mixture consisted of the following steps: (i) solubilization of sodium hydroxide (Sigma-Aldrich, 98%) in 70% of the total value of the water (Solution 1) under mechanical stirring at 400 rpm for 10 min, (ii) dissolution of methyltriethylammonium chloride - MTEACl (Sigma-Aldrich, 97%) in 30% of the water under mechanical stirring at 400 rpm for 10 min (Solution 2), (iii) mixing solutions 1 and 2 under mechanical stirring at 400 rpm for 10 min (Solution 3), (iv) addition of sodium aluminate (Merck, 53%) to solution 3 under mechanical stirring at 400 rpm for 30 min (Solution 4) and (v) addition of silica gel 60 (Fluka, 95%) to solution 4 under mechanical stirring at 400 rpm for 1 h. In the syntheses using n-butylamine (Sigma-Aldrich, 99.5%), the procedure was similar, the only difference being the addition of this amine in step (iii). The obtained gels were placed in teflon vessels, which were inserted in stainless steel autoclaves and subjected to a hydrothermal treatment under heating at 160 and 170 °C between 48 and 144 h.

The resulting solids were recovered by vacuum filtration and washed with distilled water until the supernatant reached neutral pH. Afterwards, the samples were dried in an oven at 100 °C for 24 h. Subsequently, the zeolites were subjected to a heat treatment in a muffle furnace at 550 °C for 6 h, under a heating rate of 2 °C min<sup>-1</sup>. Subsequently, the materials underwent a process of three consecutive ion exchanges at 60 °C for 3 h, using a 1.0 mol L<sup>-1</sup> ammonium chloride solution and a ratio of 1 g of zeolite per 100 mL of solution. The solids were again recovered by vacuum filtration and washed with distilled water until the supernatant reached neutral pH. Finally, the zeolites were subjected to a new heat treatment under the same conditions described above. The codes of the samples adopted in relation to the synthesis conditions are described in Table 1.

**Table 1.** Codes and synthesis conditions of the samples.

Sample	SiO <sub>2</sub> /Al <sub>2</sub> O <sub>3</sub>	MTEACl/SiO <sub>2</sub>	n-But/SiO <sub>2</sub>	Temperature (°C)
Z1	100	0.15	-	160
Z2	100	0.20	-	160
Z3	100	0.25	-	160
Z4	100	0.20	-	170
Z5	100	0.20	0.20	170
Z6	100	0.20	0.30	170

Source: Authors (2022).

### 2.2 Characterization

The X-ray diffraction analysis (XRD) was performed in a Shimadzu XRD-6000 diffractometer, CuK $\alpha$  ( $\lambda = 0.1542$  nm), Ni filter, 40 kV voltage and 30 mA current. The data was collected in the  $2\theta$  range between 3 and 40°, with goniometer velocity of 2° min<sup>-1</sup> and step of 0.02°. The area of the diffraction peaks located in the  $2\theta$  regions of 20.4° - 21.5° and 24.8° -

27.3° (Silva et al., 2017) were used to calculate the crystallinity of the materials.

Thermal analysis (TG/DTG) were performed in a Shimadzu DTG-60H thermobalance, using alumina crucibles, with a sample mass of approximately 10 mg. The analyzes took place in the range of ambient temperature to 800 °C, under a synthetic air atmosphere with a flow rate of 50 mL min<sup>-1</sup> and a heating rate of 10 °C min<sup>-1</sup>.

Nitrogen adsorption-desorption measurements were performed using a Micromeritics ASAP 2020 equipment at -196 °C, in the relative pressure range between (P/P<sub>0</sub>) between 0.01 and 0.99. The solids were previously degassed at 350 °C for 12 h, under vacuum of 2 µmHg. The specific surface area (S<sub>BET</sub>) was calculated using the BET method (Brunauer, Emmett & Teller, 1938). The microporous area (S<sub>Micro</sub>), external surface area (S<sub>Ext</sub>) and microporous volume (V<sub>Micro</sub>) were determined by the t-plot method (Lippens & De Boer, 1965). The total pore volume (V<sub>Total</sub>) was measured using the single-point BET method (Dollimore & Spooner, 1974) at P/P<sub>0</sub> = 0.995.

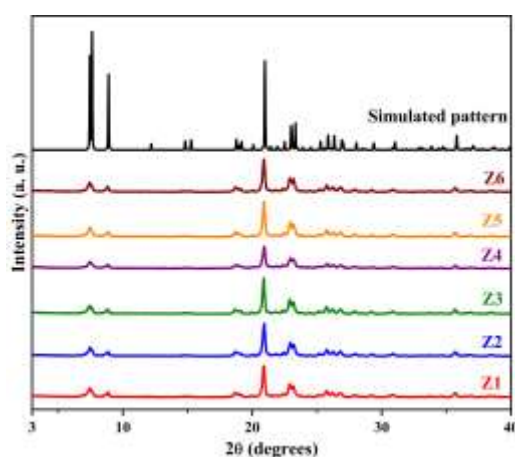
Temperature-programmed desorption of ammonia (NH<sub>3</sub>-TPD) was conducted in a multipurpose reaction system (SAMP3 model equipment, Termolab - Brazil) equipped with thermal conductivity detector. In these measurements, a mass of approximately 100 mg of sample was submitted to a pretreatment at 400 °C for 1 h, under helium atmosphere with a flow rate of 30 mL min<sup>-1</sup>. Then, the temperature was reduced to 100 °C and the sample was kept in contact with the ammonia stream at a flow rate of 30 mL min<sup>-1</sup> for 40 min. The next step of the process was the removal of the physisorbed NH<sub>3</sub> molecules at 100 °C for 1 h, under a helium flow rate of 30 mL min<sup>-1</sup>. Finally, the NH<sub>3</sub> desorption curves were obtained in the temperature range between 100 and 800 °C, with a heating rate of 10 °C min<sup>-1</sup> and under helium flow rate of 30 mL min<sup>-1</sup>.

### 3. Results and Discussion

#### 3.1 X-ray diffraction

The X-ray diffractograms of the samples as-synthesized and the simulated XRD pattern of the MTW structure (Treacy & Higgins, 2007) are shown in Figure 1. All samples denoted the presence of high intensity peaks associated to the structure of MTW (JCPDS card number 86-2364) and occurring at 2θ values of 7.4°, 7.6°, 8.9°, 20.9°, 23.0° and 23.1°, and it reveals the obtainment of the highly crystallized and phase-pure ZSM-12 when compared to the simulated pattern.

Figure 1. X-ray diffractograms.



Source: Authors (2022).

Table 2 presents the crystallization times and the relative crystallinities of the synthesized samples. The materials obtained using a temperature of 170 °C showed higher relative crystallinity values in shorter synthesis times. This is due to the fact that the increase in temperature provides a greater nucleation velocity, changing the crystal growth kinetics, and with that, allowing the formation of the MTW phase more quickly (Sanhoob et al., 2014) under the conditions studied. The simultaneous

use of methyltriethylammonium chloride and n-butylamine provided the most crystalline samples. Rollmann et al. (1999) describe that the synthesis of ZSM-12 zeolite is favored with the use of short and flexible amines, such as MTEACl and n-butylamine, acting as structure-directing agents, promoting the obtention of pure ZSM-12 zeolite and highly crystalline.

**Table 2.** Synthesis and XRD results.

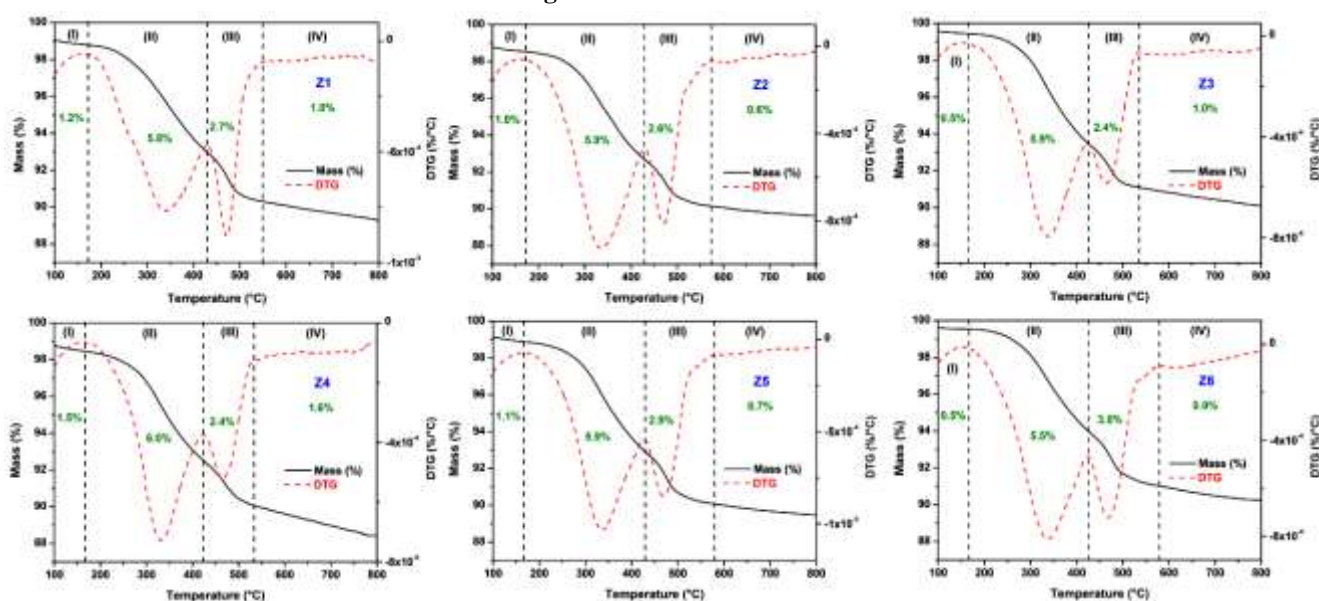
Sample	MTEACl/SiO <sub>2</sub>	n-but/SiO <sub>2</sub>	<sup>a</sup> T (°C)	<sup>b</sup> t (h)	<sup>c</sup> RC (%)
Z1	0.15	-	160	144	92
Z2	0.20	-	160	120	92
Z3	0.25	-	160	120	92
Z4	0.20	-	170	48	94
Z5	0.20	0.20	170	72	96
Z6	0.20	0.30	170	72	100

<sup>a</sup>Synthesis temperature; <sup>b</sup>Crystallization time; <sup>c</sup>Relative crystallinity. Source: Authors (2022).

### 3.2 Thermal analysis (TG/DTG)

Figure 2 shows the TG/DTG curves of the synthesized samples. Through the DTG curves, four different mass loss events were identified: (i) desorption of intracrystalline water, (ii) decomposition of the structure-directing agent diffused inside the pores of the zeolite, (iii) oxidation of the SDA strongly linked to the surface, possibly compensating for loads on the structure, (iv) removal of coke and combustion of residual amine compounds formed from the decomposition products of the structure-directing agent (Gopal et al., 2001; Santos et al., 2016). Practically all samples showed similar mass loss values for all observed events. In the case of samples Z5 and Z6, it is not possible to differentiate the decomposition of MTEACl and n-butylamine, as these events overlap. It is observed that most of the organic compounds are decomposed in event (ii), and with that, denoting a greater participation of these as pore-filling agents in relation to their performance as charge compensating counterions.

**Figure 2.** TG/DTG curves.

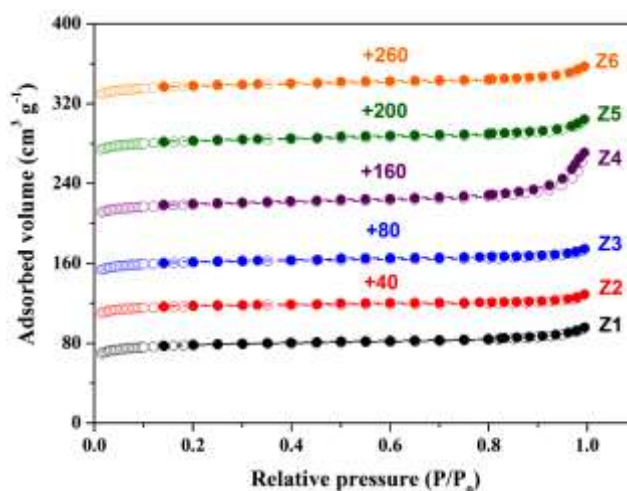


Source: Authors (2022).

### 3.3 Nitrogen Adsorption-Desorption

The nitrogen adsorption-desorption isotherms are shown in Figure 3. The samples had type I isotherms, according to the International Union of Pure and Applied Chemistry (IUPAC) classification, characteristics of purely microporous materials that have a relatively small external surface and adsorb large amounts of nitrogen at low relative pressures (Wei & Smirniotis, 2006). All samples showed the presence of type H4 hysteresis, in the  $P/P_0$  range between 0.5 and 1.0, which suggests a "pseudo" mesoporosity, this being due to the phenomenon of capillary condensation (Dimitrov et al., 2011).

**Figure 3.** Nitrogen adsorption-desorption isotherms. The isotherms of samples Z2, Z3, Z4, Z5 and Z6 were shifted by the values indicated in the figure for better visualization.



Source: Authors (2022).

Table 3 presents the textural properties of the samples obtained from nitrogen adsorption-desorption. The samples presented results very close to the area and volume values, which are consistent with those reported for the ZSM-12 zeolite (Carvalho & Urquieta-Gonzalez, 2015; Catizzone et al., 2018). The exception was the Z4 sample, which presented lower values for micropore area and volume, which we can infer a possible partial blockage of the pores by amorphous material. The use of MTEACl and n-butylamine, simultaneously, at the 0.2 ratio (sample Z5) promoted an increase in  $S_{\text{Micro}}$ , which is an improvement for the structure of ZSM-12 zeolite for its application as an adsorbent, catalyst support, among other applications.

**Table 3.** Texture properties of samples obtained from nitrogen adsorption-desorption.

Sample	$S_{\text{BET}}$ ( $\text{m}^2 \text{g}^{-1}$ )	$S_{\text{Micro}}$ ( $\text{m}^2 \text{g}^{-1}$ )	$S_{\text{Ext}}$ ( $\text{m}^2 \text{g}^{-1}$ )	$V_{\text{Total}}$ ( $\text{cm}^3 \text{g}^{-1}$ )	$V_{\text{Micro}}$ ( $\text{cm}^3 \text{g}^{-1}$ )
Z1	297	255	42	0.14	0.10
Z2	294	263	31	0.13	0.11
Z3	309	271	38	0.14	0.11
Z4	222	178	44	0.13	0.07
Z5	313	267	46	0.15	0.11
Z6	295	253	42	0.14	0.10

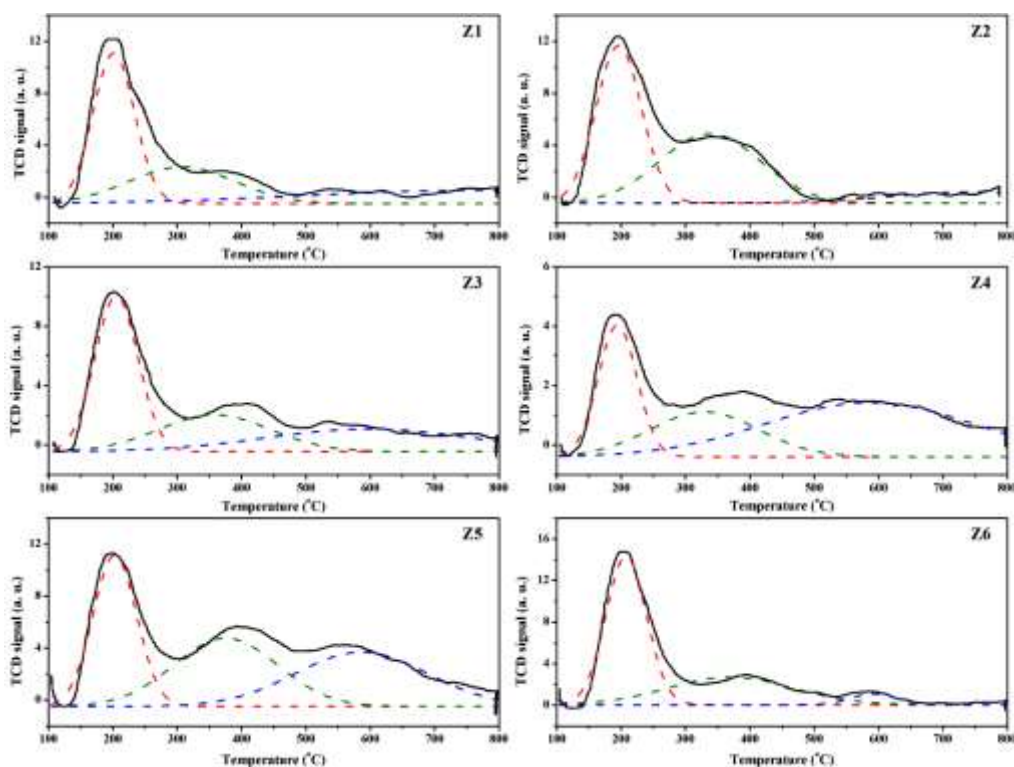
Source: Authors (2022).

### 3.4 Temperature-programmed desorption of ammonia

Figure 4 shows the  $\text{NH}_3$ -TPD profiles. All materials showed three desorption events centered around 100–300 °C,

300–500 °C and 500–800 °C, referring to ammonia desorption from the weak, medium and strong acid sites, respectively. The first, more intense event, is related to ammonia desorption from weak Brønsted acid sites and/or moderate Lewis acid sites, the second peak is described in relation to the medium Brønsted acid sites, and the third peak concerns the strong Brønsted acid sites (Lok et al., 1986).

**Figure 4.** NH<sub>3</sub>-TPD profiles.



Source: Authors (2022).

The total amounts and the distribution of acidic sites are calculated from the desorption peak area assuming the stoichiometry of one NH<sub>3</sub> molecule per acid site. The amounts of different acidic sites are summarized in Table 4. All samples showed higher density of weak acidity sites, and it can be inferred that these materials have higher extra-framework aluminum content (Li et al., 2011). The addition of another SDA promoted an increase in the total density of acidic sites (Z5 and Z6 samples) and the 0.2 ratio allowed an increase in the density of medium and strong acidic sites, indicating a greater insertion of structural aluminum in the Z5 sample compared to the others materials. The anomalous behavior of the Z4 sample could possibly be explained by the possible partial blockage of its pores, preventing access to the structure's internal acidic sites.

**Table 4.** Acid properties obtained by NH<sub>3</sub>-TPD.

Sample	Weak acid sites (μmol g <sup>-1</sup> )	Medium acid sites (μmol g <sup>-1</sup> )	Strong acid sites (μmol g <sup>-1</sup> )	Total acid sites (μmol g <sup>-1</sup> )
Z1	153	8	3	163
Z2	133	30	3	167
Z3	122	17	11	150
Z4	50	9	14	73
Z5	122	32	23	177
Z6	165	17	6	188

Source: Authors (2022).

## 4. Conclusion

A series of ZSM-12 zeolites with high crystallinity were synthesized using methyltriethylammonium chloride, individually and in conjunction with n-butylamine, as structure-directing agents. The use of two SDAs promoted an increase in crystallinity. Thermal analysis denoted that most of MTEACl and n-butylamine act as pore-filling agents. The samples showed isotherms characteristic of microporous ZSM-12 zeolite. The materials presented a higher density of weak acidity sites, indicating the presence of higher extra-framework Al content. The anomalous results presented by the Z4 sample of the textural properties and acidity indicate a possible partial blockage of the pores of this zeolite. The simultaneous use of SDAs in the 0.2 ratio (Z5 sample) promoted an increase in the microporous area and in the densities of medium and strong acid sites, showing an improvement in the zeolite structure.

As suggestions for future work, we propose to study the effect of the individual and simultaneous use of other structure directing agents used in the synthesis of ZSM-12, such as tetraethylammonium hydroxide (TEAOH) and hexamethyleneimine (HMI), on the textural and acidic properties of the zeolite, and to evaluate the effect of performing post-synthesis treatments (dealumination and desilication) on the physicochemical characteristics of ZSM-12 obtained from the use of mono or dual-template.

## References

- Barrer, R. M. (1948). Synthesis of a zeolitic mineral with chabazite-like sorptive properties, *Journal of the Chemical Society*, 2, 127–132. <https://doi.org/10.1039/JR9480000127>
- Cao, P., Li, B., Sun, W. & Zhao, L. (2021). Understanding the Zeolites Catalyzed Isobutane Alkylation based on Their Topology Effects on the Reactants Adsorption, *Chemical Engineering Science*, 250, 117387. <https://doi.org/10.1016/j.ces.2021.117387>
- Carvalho, K. T. G. & Urquieta-Gonzalez, E. A. (2015). Microporous–mesoporous ZSM-12 zeolites: Synthesis by using a soft template and textural, acid and catalytic properties, *Catalysis Today*, 243, 92-102. <https://doi.org/10.1016/j.cattod.2014.09.025>
- Catizzone, E., Cirelli, Z., Aloise, A., Lanzafame, P., Migliori, M. & Giordano, G. (2018). Methanol conversion over ZSM-12, ZSM-22 and EU-1 zeolites: from DME to hydrocarbons production, *Catalysis Today*, 304, 39-50. <https://doi.org/10.1016/j.cattod.2017.08.037>
- Chen, Y., Li, C., Chen, X., Liu, Y. & Liang, C. (2018). Synthesis of ZSM-23 zeolite with dual structure directing agents for hydroisomerization of n-hexadecane, *Microporous and Mesoporous Materials*, 268, 216-224. <https://doi.org/10.1016/j.micromeso.2018.04.033>
- Chokkalingam, A., Kawagoe, H., Watanabe, S., Moriyama, Y., Komura, K., Kubota, Y., Kim, J.-H., Seo, G., Vinu, A. & Sugi, Y. (2013). Isopropylation of biphenyl over ZSM-12 zeolites, *Journal of Molecular Catalysis A: Chemical*, 367, 23-30. <https://doi.org/10.1016/j.molcata.2012.10.018>
- Dimitrov, L., Mihaylov, M., Hadjiivanov, K. & Mavrodinova, V. (2011). Catalytic properties and acidity of ZSM-12 zeolite with different textures, *Microporous and Mesoporous Materials*, 143(2-3), 291-301. <https://doi.org/10.1016/j.micromeso.2011.03.009>
- Figueiredo, B. R., Cardoso, S. P., Portugal, I., Rocha, J., Silva, C. M. (2018). Inorganic Ion Exchangers for Cesium Removal from Radioactive Wastewater, *Separation & Purification Reviews*, 47(4), 306-336. <https://doi.org/10.1080/15422119.2017.1392974>
- Gopal, S., Yoo, K. & Smirniotis, P. G. (2001). Synthesis of Al-rich ZSM-12 using TEAOH as template, *Microporous and Mesoporous Materials*, 49(1-3), 149-156. [https://doi.org/10.1016/S1387-1811\(01\)00412-7](https://doi.org/10.1016/S1387-1811(01)00412-7)
- Glotov, A., Demikhova, N., Rubtsova, M., Melnikov, D., Tsaplin, D., Gushchin, P., Egazar'yants, S., Maximov, A., Karakhanov, E. & Vinokurov, V. (2021). Bizeolite Pt/ZSM-5:ZSM-12/Al<sub>2</sub>O<sub>3</sub> catalyst for hydroisomerization of C-8 fraction with various ethylbenzene content, *Catalysis Today*, 378, 83-95. <https://doi.org/10.1016/j.cattod.2021.02.008>
- Han, B., Lee, S.-H., Shin, C.-H., Cox, P. A. & Hong, S. B. (2005). Zeolite Synthesis Using Flexible Diquaternary Alkylammonium Ions (C<sub>n</sub>H<sub>2n+1</sub>)<sub>2</sub>NH<sup>+</sup>(CH<sub>2</sub>)<sub>5</sub>N<sup>+</sup>H(C<sub>n</sub>H<sub>2n+1</sub>)<sub>2</sub> with n = 1–5 as Structure-Directing Agents, *Chemistry of Materials*, 17(3), 477–486. <https://doi.org/10.1021/cm048418+>
- Holland, B. T., Abrams, L. & Stein, A. (1999). Dual Templating of Macroporous Silicates with Zeolitic Microporous Frameworks, *Journal of the American Chemical Society*, 121(17), 4308–4309. <https://doi.org/10.1021/ja990425p>
- Imyen, T., Saenluang, K., Dugkhuntod, P. & Wattanakit, C. (2021). Investigation of ZSM-12 nanocrystals evolution derived from aluminosilicate nanobeads for sustainable production of ethyl levulinate from levulinic acid esterification with ethanol, *Microporous and Mesoporous Materials*, 312, 110768. <https://doi.org/10.1016/j.micromeso.2020.110768>
- Kasunič, M., Legiša, J., Meden, A., Loga, N. Z., Beale, A. M. & Golobič, A. (2009). Crystal structure of pure-silica ZSM-12 with tetraethylammonium cations from X-ray powder diffraction data, *Microporous and Mesoporous Materials*, 122(1-3), 255-263. <https://doi.org/10.1016/j.micromeso.2009.03.008>

- Kore, R. & Srivastava, R. (2012). Synthesis of zeolite Beta, MFI, and MTW using imidazole, piperidine, and pyridine based quaternary ammonium salts as structure directing agents, *RSC Advances*, 2(26), 10072-10084. <https://doi.org/10.1039/C2RA20437A>
- Kosareva, Gerasimov, D. N., Maslov, I. A., Pigoleva, I. V., Zaglyadova, S. V. & Fadeev, V. V. (2021). Effect of the Zeolite Type on Catalytic Performance in Dewaxing of the Diesel Fraction under Sour Conditions, *Energy & Fuels*, 35(19), 16020-16034. <https://doi.org/10.1021/acs.energyfuels.1c01484>
- Kulikov, L. A., Tsaplin, D. E., Knyazeva, M. I., Levin, I. S., Kardashev, S. V., Filippova, T. Y., Maksimov, A. L. & Karakhanov, E. A. (2019). Effect of Template Structure on the Zeolite ZSM-12 Crystallization Process Characteristics, *Petroleum Chemistry*, 59(S1), S60-S65. <https://doi.org/10.1134/S0965544119130097>
- Kwon, S., Kim, C., Han, E., Lee, H., Cho, H. S. & Choi, M. (2021). Relationship between zeolite structure and capture capability for radioactive cesium and strontium, *Journal of Hazardous Materials*, 408, 124419. <https://doi.org/10.1016/j.jhazmat.2020.124419>
- Lee, H. J., Kim, S. H., Kim, J. H., Park, S. J. & Cho, S. J. (2014). Synthesis and characterization of zeolites MTT and MFI, with controlled morphologies using mixed structure directing agents, *Microporous and Mesoporous Materials*, 195, 205-215. <https://doi.org/10.1016/j.micromeso.2014.04.035>
- Li, C., Li, L., Wu, W., Wang, D., Toktarev, A. V., Kikhtyanin, O. V. & Echevskii, G.V. (2011). Highly selective synthesis of 2,6-dimethylnaphthalene over alkaline treated ZSM-12 zeolite, *Procedia Engineering*, 18, 200-205. <https://doi.org/10.1016/j.proeng.2011.11.032>
- Li, J., Lou, L.-L., Xu, C. & Liu, S. (2014). Synthesis, characterization of Al-rich ZSM-12 zeolite and their catalytic performance in liquid-phase tert-butylation of phenol, *Catalysis Communications*, 50, 97-100. <https://doi.org/10.1016/j.catcom.2014.03.011>
- Lok, B. M., Marcus, B. K. & Angell, C. L. (1986). Characterization of zeolite acidity. II. Measurement of zeolite acidity by ammonia temperature programmed desorption and FT-IR Spectroscopy techniques. *Zeolites*, 6(3), 185-194. [https://doi.org/10.1016/0144-2449\(86\)90046-1](https://doi.org/10.1016/0144-2449(86)90046-1)
- Masoumifard, N., Kaliaguine, S. & Kleitz, F. (2016). Synergy between structure direction and alkalinity toward fast crystallization, controlled morphology and high phase purity of ZSM-12 zeolite, *Microporous and Mesoporous Materials*, 227, 258-271. <https://doi.org/10.1016/j.micromeso.2016.02.044>
- Margarit, V. J., Martínez-Armero, M. E., Navarro, M. T., Martínez, C. & Corma, A. (2015). Direct Dual-Template Synthesis of MWW Zeolite Monolayers, *Angewandte Chemie International Edition*, 54(46), 13724-13728. <https://doi.org/10.1002/anie.201506822>
- Mehla, S., Krishnamurthy, K. R., Viswanathan, B., John, M., Niwate, Y., Kumar, S. A. K., Pai, S. M. & Newalkar, B. L. (2013). n-Hexadecane hydroisomerization over BTMACI/TEABr/MTEABr templated ZSM-12, *Microporous and Mesoporous Materials*, 177, 120-126. <https://doi.org/10.1016/j.micromeso.2013.05.001>
- Milton, R. M. (1959). Molecular sieve adsorbents, U.S. pat. 2,882,243.
- Moini, A., Schmitt, K. D., Valyocsik, E. W. & Polomski, R. F. (1994). The Role of Diquaternary Cations as Directing Agents in Zeolite Synthesis, *Studies in Surface Science and Catalysis*, 84, 23-28. [https://doi.org/10.1016/S0167-2991\(08\)64075-6](https://doi.org/10.1016/S0167-2991(08)64075-6)
- Počkaj, M., Meden, A., Logar, N. Z., Rangus, M., Mali, G., Lezcano-Gonzalez, I., Beale, A. M. & Golobič, A. (2018). Structural investigations in pure-silica and Al-ZSM-12 with MTEA or TEA cations, *Microporous and Mesoporous Materials*, 263, 236-242. <https://doi.org/10.1016/j.micromeso.2017.12.015>
- Rani, P., Srivastava, R. & Satpati, B. (2016). One-Step Dual Template Mediated Synthesis of Nanocrystalline Zeolites of Different Framework Structures, *Crystal Growth & Design*, 16(6), 3323-3333. <https://doi.org/10.1021/acs.cgd.6b00299>
- Rodeghero, E., Pasti, L., Nunziante, G., Chenet, T., Gigli, L., Plaisier, J. R. & Martucci, A. (2019). Highlighting the capability of zeolites for agro-chemicals contaminants removal from aqueous matrix: Evidence of 2-ethyl-6-methylaniline adsorption on ZSM-12, *American Mineralogist*, 104(3), 317-324. <https://doi.org/10.2138/am-2019-6754>
- Rollmann, L. D., Schlenker, J. L., Lawton, S. L., Kennedy, C. L., Kennedy, G. J. & Doren, D. J. (1999). On the Role of Small Amines in Zeolite Synthesis, *The Journal of Physical Chemistry B*, 103(34), 7175-7183. <https://doi.org/10.1021/jp991913m>
- Rosinski, E. J. & Rubin, M. K. (1974). Crystalline Zeolite ZSM-12, U.S. Patent 3 832 449.
- Sanhoob, M., Muraza, O., Yamani, Z. H., Al-Mutairi, E. M., Tago, T., Merzougui, B. & Masuda, T. (2014). Synthesis of ZSM-12 (MTW) with different Al-source: Towards understanding the effects of crystallization parameters, *Microporous and Mesoporous Materials*, 194, 31-37. <https://doi.org/10.1016/j.micromeso.2014.03.033>
- Sanhoob, M. A., Muraza, O., Yoshioka, M., Qamaruddin, M. & Yokoi, T. (2018). Lanthanum, cerium, and boron incorporated ZSM-12 zeolites for catalytic cracking of n-hexane, *Journal of Analytical and Applied Pyrolysis*, 129, 231-240. <https://doi.org/10.1016/j.jaap.2017.11.007>
- Santos, M. R. F., Pedrosa, A. M. G. & Souza, M. J. B. (2016). Oxidative desulfurization of thiophene on TiO<sub>2</sub>/ZSM-12 zeolite, *Materials Research*, 19(1), 24-30. <https://doi.org/10.1590/1980-5373-MR-2015-0130>
- Silva, A. O. S., Souza, M. J. B., Pedrosa, A. M. G., Coriolano, A. C. F., Fernandes Jr. V. J. & Araujo, A. S. (2017). Development of HZSM-12 zeolite for catalytic degradation of high-density polyethylene, *Microporous and Mesoporous Materials*, 244, 1-6. <https://doi.org/10.1016/j.micromeso.2017.02.049>
- Toktarev, A. V. & Ione, K. G. (1997). Studies on crystallization of ZSM-12 type zeolite, *Studies in Surface Science and Catalysis*, 105, 333-340. [https://doi.org/10.1016/S0167-2991\(97\)80573-3](https://doi.org/10.1016/S0167-2991(97)80573-3)
- Treacy, M. M. J. & Higgins, J. B. (2007). Collection of Simulated XRD Powder Patterns for Zeolites, (5th. ed.), Elsevier.
- Vesely, O., Pang, H., Vornholt, S. M., Mazur, M. & Yu, J. (2019). Opanasenko, M., Eliášová, P. Hierarchical MTW zeolites in tetrahydropyranlation of alcohols: Comparison of bottom-up and top-down methods, *Catalysis Today*, 324, 123-134. <https://doi.org/10.1016/j.cattod.2018.06.010>

Wang, B., Tian, Z., Li, P., Wang, L., Xu, Y., Qu, W., Ma, H., Xu, Z. & Lin, L. (2009). Synthesis of ZSM-23/ZSM-22 intergrowth zeolite with a novel dual-template strategy, *Materials Research Bulletin*, 44(12), 2258-2261. <https://doi.org/10.1016/j.materresbull.2009.07.017>

Wei, X. & Smirniotis, P. G. (2006). Development and characterization of mesoporosity in ZSM-12 by desilication, *Microporous and Mesoporous Materials*, 97(1-3), 97-106. <https://doi.org/10.1016/j.micromeso.2006.01.024>